

TEMPERATURE AND MECHANICAL STRESS MONITORING OF HIGH VOLTAGE CABLES USING FIBER-BRAGG GRATINGS

Fikri Serdar GÖKHAN

Uludag University
Engineering and Architecture Faculty
Electronics Engineering
E-mail: fsgokhan@uludag.edu.tr

Güneş YILMAZ

TURK PIRELLI Cable and Systems
R&D Department
Mudanya /Bursa
E-mail: gunes.yilmaz@tr.pirelli.com

Abstract—To be able to confidently use High Voltage cables under all circumstances up to their design transmission capacity, temperature monitoring systems are being installing in order to predict maximal conductor temperature of a dynamic rating system. Generally, monitoring systems are focused at DTS fiber sensors (Distributed temperature Sensing) which uses the dependence of Raman scattering on temperature changes. This paper presents a new fiber Bragg grating sensor configuration for simultaneous Measurement of Strain and temperature for High Voltage (HV) cables using Fiber Bragg Gratings. By using number of sensor heads each measuring a different temperature and mechanical stress (strain) locally , a long distance monitoring could be established.

Index Terms— High Voltage Cable Network, Thermo-mechanical Stresses, fiber Bragg gratings, fiber optic sensors.

I. INTRODUCTION

The prime aging stresses that may induce aging in polyethylene cables are electrical, thermal and mechanical in nature. For thermal stress, the maximum temperature, temperature gradient and the extreme limits of the ambient temperature influence the aging rate [1]. In the case of mechanical stress, the bending tension, pressure, cyclic compression and torsion stresses will exert varied aging influences. The environmental sub variables affecting aging are composition of the ambient gases (e.g. air, oxygen, nitrogen and low molecular weight hydrocarbons), presence of lubricants, water or humidity, corrosive chemicals and ionizing and ultra – violet radiation.

As a consequence of the elevated power loads, the insulating system of an XLPE transmission cable will be subjected to high temperatures and a temperature gradient. The maximum permissible temperature, which occurs adjacent to conductor, has been set by the IEC 287 Specifications to 90°C for continuous and to 130°C for emergency operation. The maximum temperature, temperature gradient and the extreme limits of the ambient temperature influence the aging rate of insulation. Tests show that the crystalline regions of XLPE melt over a relatively wide temperature regime (60 to 90°C). For XLPE at 90°C the ac and impulse breakdown values are reduced by 6 and 19% respectively

from those at room temperature, with further respective reductions of 18 and 48% at 115°C. This requires careful determination of maximum operating temperature and the emergency temperature limit of 130°C. In addition at 130°C the depressed value of the mechanical modules forebodes the possibility of thermomechanical damage. It is known that exposure of XLPE above 150°C can generate water from cumyl alcohol decomposition, one of the cross-linking products of dicumyl peroxide. Such temperatures are often reached during molding of splice joints where the water condenses to form microcavities during cooling stage from these high temperatures; both water content and the number of voids increase with the amount of antioxidant and oxygen in polymer. The presence of water- filled cavities could lead to water or electrical trees during cable operation, thereby increasing the probability of eventual insulation failure. Therefore, the feasibility of limiting the emergency temperature to the melting point (105 °C) or even lower is very important to continue service of HV cables.

II. MONITORING HV CABLE NETWORK USING FIBER BRAGG GRATINGS

In recent years, a considerable number of techniques for temperature and mechanical stresses monitoring of High Voltage cables based on fiber sensors have been proposed and demonstrated. Traditionally, DTS sensors are being proposed by several cable designers in HV cable network monitoring. In this study we investigate monitoring HV cable network using Fiber Bragg gratings. In a letter by Cavaleiro, *et al.* [2], a fiber sensor was presented using two superimposed fiber Bragg gratings written at different wavelengths in order to obtain distinct temperature and strain sensitivities. Some disadvantages related to the previous reported techniques for temperature/strain discrimination can be overcome by using a Bragg grating simultaneously sensitive to temperature and strain and an additional strain-immune grating as a temperature reference. However, in order to implement this technique, proper mechanical protection of the reference grating is needed, which can lead to practical constrains in the process of embedding the sensor.

In this study , monitoring HV Cables using sensor that is suitable for simultaneous measurement of strain and temperature over XLPE is investigated. The fiber

used in sensing temperature and mechanical strain of HV cable has number of individual sensor heads. These sensors have two gratings with close wavelengths written and separated identically in two spliced sections of germanosilicate fibers and one of the germanosilicate fiber is codoped with boron. Therefore, a small sensing element with two Bragg gratings of similar strain sensitivities but different responses to temperature of XLPE insulation can be constructed.

III. THEORY

The geometry of the proposed sensor that is used to determine temperature and strain variations of High Voltage cables is shown in Fig. 1. The change in temperature and strain of the insulation XLPE cause shift in Bragg wavelengths as

$$\Delta\lambda_{Bi} = K_{Ti}\Delta T + K_{\epsilon i}\Delta\epsilon \quad (1)$$

where $i=1,2$ represent the grating written in the germanosilicate fiber and in the boron-codoped-germanosilicate fiber, respectively. The thermal sensitivity, K_{Ti} , depends on the thermal expansion of the fiber *i.e.*, thermo-optic coefficient.

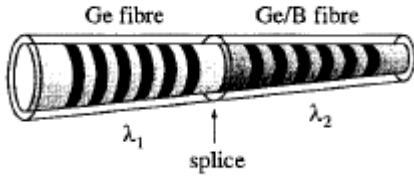


Fig.1 Sensor head geometry

During Fabrication of the grating at an elevated temperature T_w , the Bragg wavelength will be defined by the period, Λ_g of the grating. After fabrication, when the temperature is returned to a final temperature T_f , the Bragg wavelength will be

$$\lambda_{Bragg} = 2\Lambda_g \left(1 + \alpha[T_f - T_w] + \frac{dn_{eff}}{dT}[T_f - T_w] \right) \quad (2)$$

where α is thermal expansion coefficient of the fiber and dn_{eff}/dT is the temperature coefficient of the mode index. This is merely the change in the refractive index of the fiber core as a function of temperature.[3] This equation may be simplified by expanding and rearranging to :

$$\lambda_{Bragg} = 2\Lambda_g \left(n_{eff} \left(1 + \alpha[T_f - T_w] + \frac{dn_{eff}}{dT}[T_f - T_w] \right) \right) \quad (3)$$

The thermal expansion of silica is approximately $5,2 \times 10^{-7}$, whereas $dn_{eff}/dT \approx +1,1 \times 10^{-5} \text{ } ^\circ\text{C}^{-1}$, the contribution of the thermal expansion coefficient term is approximately 10% in comparison. This equation is further simplified to ;

$$\lambda_{Bragg} = \underbrace{2\Lambda_g n_{eff}}_{\lambda_{BRAGG}} [1 + \alpha \cdot \Delta T] + 2\Lambda_g \frac{dn_{eff}}{dT} [T_f - T_w] \quad (4)$$

$$\lambda_{Bragg} - 2\Lambda_g n_{eff} [1 + \alpha \cdot \Delta T] = 2\Lambda_g \frac{dn_{eff}}{dT} \Delta T \quad (5)$$

$$\Delta\lambda_{BRAGG} = \underbrace{2\Lambda_g \frac{dn_{eff}}{dT}}_{K_T} \Delta T \quad (6)$$

On the other hand, the strain sensitivity, $K_{\epsilon i}$, depends on the photoelastic coefficient of the fiber, but is mainly determined by the variation of the grating pitch with the applied strain, which depends on the mechanical properties of the fiber.

IV. STRAIN RESPONSE OF BRAGG GRATINGS

To shift the Bragg grating central wavelength peak, mechanical stresses have been applied to the optical fiber. In particular, the shift range is directly proportional to the fiber Bragg grating strain. Therefore, due to the silica Poisson ratio, $\nu=0.17$, axial strains, ϵ_z , in comparison with radial, $\epsilon_r = -\nu \cdot \epsilon_z$, have been applied to the fiber. Furthermore, due to the better resistance properties of silica under compression than under tension applied to fibers [4]. The relationship between the stress and the strain for a material in the elastic domain and in the axial direction Z is given by

$$\sigma_Z = E \cdot \epsilon_Z \quad (7)$$

where $E=7.25 \times 10^4 \text{ N/mm}^2$ is the silica Young modulus and ϵ_Z is the axial strain which is defined by ;

$$\epsilon_z = \frac{\Delta L_Z}{L_Z} \quad (8)$$

where ΔL_Z is the axial displacement and is the stressed length (Fig. 2).

The shift of the Bragg central wavelength peak, $\Delta\lambda$ is related to the effective refractive index change, Δn and the change in the grating period, Λ , by the following relationship:

$$\frac{\Delta\lambda}{\lambda} = \frac{\Delta\Lambda}{\Lambda} + \frac{\Delta n}{n} \quad (9)$$

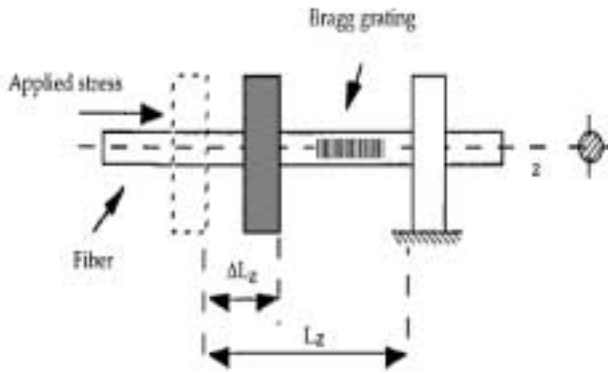


Fig.2 Concept of axial Compression

Resolving this equation in terms of transversal (T) and axial (Z) strain we obtain, neglecting thermal effects ;

$$\frac{\Delta\lambda}{\lambda} = \varepsilon_Z - \frac{n^2}{2} \cdot [p_{11} \cdot \varepsilon_T + p_{12} \cdot (\varepsilon_T + \varepsilon_Z)] \quad (10)$$

where p_{ij} are the photoelastic constants of the strain optic tensor. This equation for an isotropic and homogeneous material , can be simplified as follows:

$$\frac{\Delta\lambda}{\lambda} = (1 - p_e) \cdot \varepsilon_Z \quad (11)$$

where $p_e=0.21$ is the photoelastic coefficient.

Thus, a wavelength shift $\Delta\lambda$ could be obtained imposing a strain to an optical fiber. In particular, the wavelength shift is negative for compressive strains and positive for tensile strains.

It is known that the presence of boron in the core of optical fiber leads to a decrease of the refractive index and decrease in thermo-optic coefficient. Therefore, the temperature dependence of the Bragg wavelength can be modified by boron codoping of germanosilicate fiber. Considering the fact that boron codoping has no observable effect on the mechanical properties of the fiber, we can conclude that, in general, $K_{T1} \neq K_{T2}$ and $K_{\varepsilon1} = K_{\varepsilon2}$. In this way, (1) can be used to discriminate between temperature and strain effects applied to the sensor head:

$$\begin{bmatrix} \Delta T \\ \Delta \varepsilon \end{bmatrix} = \frac{1}{\Delta} \begin{bmatrix} K_{\varepsilon2} & -K_{\varepsilon1} \\ -K_{T2} & K_{T1} \end{bmatrix} \begin{bmatrix} \Delta\lambda_{B1} \\ \Delta\lambda_{B2} \end{bmatrix} \quad (12)$$

where $\Delta = K_{T1} K_{\varepsilon2} - K_{\varepsilon1} K_{T2}$. Clearly, the efficiency of the method depends on the difference between K_{T1} and K_{T2} , which is determined by the concentration of boron in the codoped germanosilicate fiber.

V. SIMULATION OF EXPERIMENT AND DISCUSSION

The scheme of the HV cable network including sensor heads is shown in Fig.3. For the propose of experimental demonstration, in the grating fabrication process germanosilicate fiber is written with $\lambda_{B1} \approx 1285$ nm and codoped germanosilicate fiber is written with $\lambda_{B2} \approx 1280$ nm and more than 95% reflectivity. For the second sensor head $\lambda_{B1} \approx 1295$ nm $\lambda_{B2} \approx 1290$ nm and for third sensor head $\lambda_{B1} \approx 1305$ nm and $\lambda_{B2} \approx 1300$ nm and so on. For monitoring 5 km of HV cable network, measuring

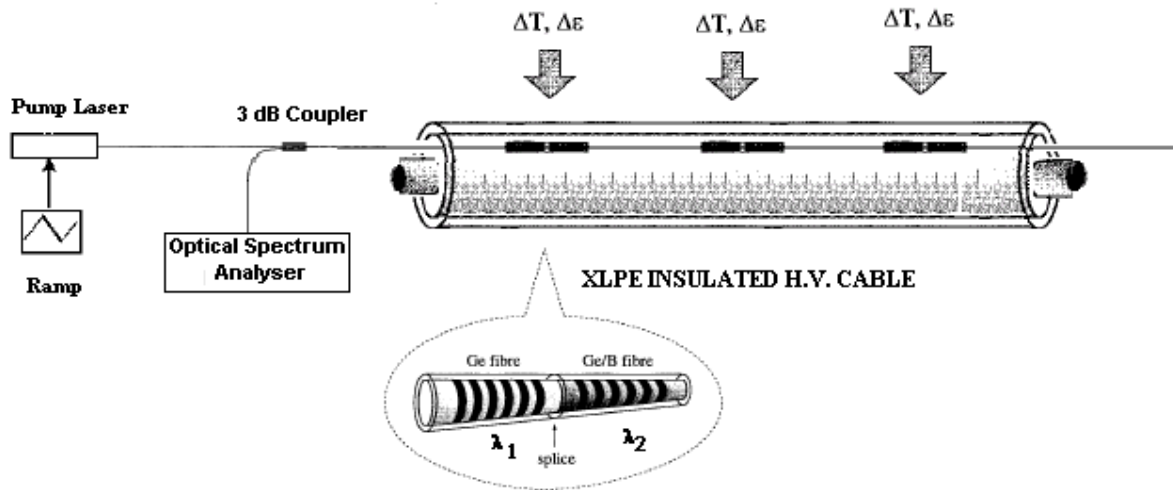


Fig 3. Monitoring HV cable with the sensor head geometry

point at each 200 m, 25 sensor head are required [5]. The gratings were thermally annealed and spliced close to each other, resulting in a sensor head with total length $L < 10$ mm. This short length ensures single-mode operation of the grating in the boron codoped fiber, although its cut-off wavelength is 1402 nm. Since the geometry and numerical aperture of the two fibers are identical, a standard low loss splice could be achieved (insertion loss < 0.02 dB). These sensor heads were then placed in a 200 m long HV cable spaced with 10 m and

the HV cable is simultaneously subjected to axial strain variations. As shown in Fig. 3, the gratings were illuminated with a pump laser (λ_0 ranges 1280-1350 nm), and an optical spectrum analyzer was used to measure the induced central wavelength shifts of the reflected peaks. Figs. 4 and 5 show the measured reflection spectra responses of the two sensing heads to applied temperature and strain variations, respectively.

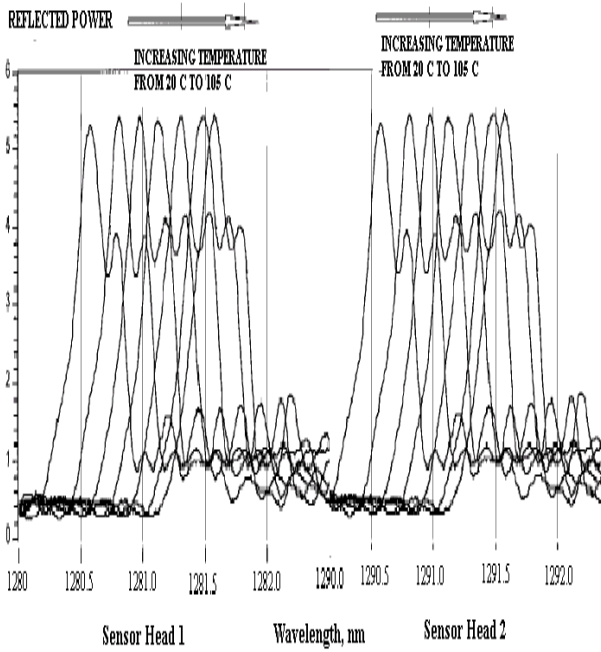


Fig. 4. Measured reflection spectra of the sensor head under different insulation temperature

For the first sensor head, calculated thermo-optic and photoelastic coefficients are as follows;

$$\Delta\lambda_{BRAGG} = 2\Lambda_g \underbrace{\frac{dn_{eff}}{dT}}_{K_T} \Delta T \quad (13)$$

$$\Lambda_g = \frac{\lambda_{BRAGG}}{2n_{eff}} \quad (14)$$

$$\Delta\lambda_{BRAGG} = 2\Lambda_g \frac{dn_{eff}}{dT} \Delta T \quad (15)$$

$$\Delta\lambda_{BRAGG} = \frac{\lambda_{BRAGG}}{n_{eff}} \frac{dn_{eff}}{dT} \Delta T \quad (16)$$

$$n_{eff} = 1,46$$

For Germanosilicate core $\lambda_{BRAGG}=1285$ nm

$$\text{And } \frac{dn_{eff}}{dT} = 1,1 \times 10^{-5} C^{-1} \quad (17)$$

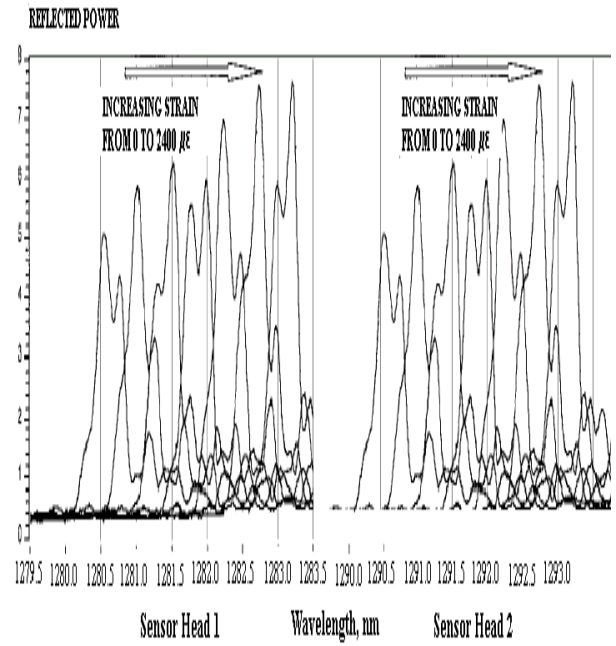


Fig. 5 . Measured reflection spectra of the sensor head under different strain (mechanical stress)

For Boron-Germanosilicate core $\lambda_{BRAGG}=1280$ nm

$$\text{And } \frac{dn_{eff}}{dT} = 1,06 \times 10^{-5} C^{-1} \quad (18)$$

$$K_{T1} = \frac{1285nm}{1,46} \times 1,1 \times 10^{-5} C^{-1} = 96,8 \times 10^{-4} nm/^{\circ}C$$

$$K_{T2} = \frac{1280nm}{1,46 - 10^{-4}} \times 1,06 \times 10^{-5} C^{-1} = 92,9 \times 10^{-4} nm/^{\circ}C \quad (19)$$

$$\frac{\Delta\lambda}{\lambda} = (1 - p_e) \cdot \epsilon_Z \quad (20)$$

$$\Delta\lambda = \underbrace{(1 - p_e) \cdot \lambda \cdot \epsilon_Z}_{K_e}$$

$$p_e = 0,21$$

$$K_{\epsilon 1}=0,79 \times 1285 \text{ nm} \times 10^{-6} / \mu \epsilon = 10,15 \times 10^{-4} \text{ nm} / \mu \epsilon$$

$$K_{\epsilon 2}=0,79 \times 1280 \text{ nm} \times 10^{-6} / \mu \epsilon = 10,11 \times 10^{-4} \text{ nm} / \mu \epsilon \quad (21)$$

Substitution of the obtained coefficients in (12) yields

$$\begin{bmatrix} \Delta T \\ \Delta \epsilon \end{bmatrix} = 280 \begin{bmatrix} 10,11 & -10,15 \\ -92,9 & 96,8 \end{bmatrix} \begin{bmatrix} \Delta \lambda_{B1} \\ \Delta \lambda_{B2} \end{bmatrix} \quad (22)$$

By using equation (3) and data from the optical spectrum analyzer output, we can predict strain and temperature simultaneously applied to the sensor head. In the measurement range of 105 °C and 0,8mε, the maximum experimental errors obtained were within ±2,2 °C and ±18,4 με. If the germanosilicate fibers are codoped with higher levels of boron, better resolution can be achieved, although the attenuation of particular sensor heads will increase.

Since the cut-off wavelength of boron codoped fiber is 1402 nm, the number of sensor heads are limited. Also the attenuation of particular gratings limit the monitoring distance of HV cables since in the frequency range between 1280 and 1402 limited number of sensor heads can be placed. And also mechanical strength of the fusion splice between similar fibers must be identical with the boron-codoped / germanosilicate fiber and the splice must be low-loss. It is of particular importance to note that the strain/temperature discrimination is based on difference in thermal sensitivities of the sensing gratings.

IV. CONCLUSION

For monitoring of HV Cables we have presented a technique based on the usage of Fiber Bragg Gratings. By using fiber sensor head that consists of two Bragg gratings written in germanosilicate core and boron-codoped germanosilicate core fibers, simultaneously induced strain and temperature can be monitored over the length of HV cable. The design uses more than one sensor heads to monitor local hot spots and mechanical stress of HV cable.

REFERENCES

- [1] R.J. Densley, R. Bartnikas and B. Bernstein, "Multiple Stress of Solid -Dielectric Extruded Dry-Cured Insulation Systems for Power Transmission Cables" in *Proc.IEEE Transactions on Power Delivery*, Vol. 9, No 1, January 1994 pp. 559 – 571.
- [2] P. M. Cavaleiro, F.M. Araujo, L. A. Ferreira, J. L. Santos, F.Farahi "Simultaneous Measurement of Strain and Temperature Using Bragg Gratings Written in Germanosilicate and Boron-Codoped Germanosilicate Fibers" *IEEE Photonics Technology Letters* 11.12 (Dec. 1999 [PTL]): 1635-1637.
- [3] R.Kashyap "Fiber Bragg Gratings" Academic Press 1999 pp. 89-90
- [4] A. Iocco, H.G. Limberger, R.P. Salathe, L.A. Everall, K.E. Chisholm, J.A.R. Williams and I.Bennion. "Bragg grating fast tunable filter for wavelength division multiplexing." *Journal of Lightwave Technology* 17.7 (Jul. 1999 [J-LT]): 1217-1221.
- [5] G. Balog, T.I. Nerby, E. KaldHussaeter, Alcatel Kabel Norge, Halden, Norway "Cable temperature Monitoring" Fifth International Conference on Insulated Power cables 20-24 June 1999- Versailles-France pp.581